

A Coupled Mathematical Model of Cell Migration, Vessel Cooption and Tumour Microenvironment during the Initiation of Micrometastases

Yan Cai^{1,2,3}, Jie Wu⁴, Zhiyong Li^{1,2}

Abstract: We propose a coupled mathematical model for the detailed quantitative analyses of initial microtumour and micrometastases formation by including cancer cell migration, host vessel cooption and changes in microenvironment. Migrating cells are included as a new phenotype to describe the migration behaviour of malignant tumour cells. Migration probability of a migrating cell is assumed to be influenced by local chemical microenvironment. Pre-existing vessel cooption and remodelling are introduced according to the local haemodynamical microenvironment, such as interstitial pressure and vessel wall permeability. After the tumour cells and tumour vessels distribution are updated, the chemical substances are coupled calculated with the haemodynamical environment. The simulation results clearly reproduce the tumour cells migrate and proliferate along the pre-existing vessels at the very early stage of growth, which are consistent with many published experimental observations. In addition, the model demonstrates the interactions of tumour cells with the pre-existing vessels, which are believed to be essential for initial adhesion, proliferation, invasion, and micrometastases establishment. Quantitative analysis of tumour expansion in longitudinal and transverse directions shows that the cooption and migration along host vessels will be inhibited once angiogenesis phase occurs. The influences of the ability of cell migration and the inclusion of vessel cooption on the formation of micrometastases are discussed.

Keywords: tumour micrometastases; vessel cooption; microenvironment; mathematical modelling

¹ State Key Laboratory of Bioelectronics, Southeast University, Nanjing, 210096, China

² School of Biological Science and Medical Engineering, Southeast University, Nanjing, 210096, China

³ Corresponding author, 86 25 83796220, Email: yancai@seu.edu.cn.

⁴ School of Naval Architecture, Ocean and Civil Engineering, Shanghai Jiaotong University, Shanghai, 200240, China

1 Introduction

Metastasis is responsible for most cancer deaths. Unfortunately, tumour metastases are very difficult to detect in cancer patients and traditional animal models. This is partly due to the challenges in the establishment of specialized animal models and imaging techniques that allow efficient and detailed *in vivo* analysis of individual cells. Most of our knowledge of the initial formation of micrometastases is deduced from static images captured from late stage of tumour progression. The interactions of tumour cells with host vessels and microenvironment are still currently not fully understood, especially at the earliest stage of micrometastases formation.

It has been generally accepted that most tumours and metastases initiate as small avascular masses, then induce angiogenesis due to hypoxic microenvironment once they grow to a few millimeters in size [Folkman (1971, 2003)]. This classic concept has been challenged by some studies which suggest that tumour cells may coopt pre-existing blood vessels at the early growth, without inducing angiogenesis in a vascularized tissue [Holash, Maisonpierre, Compton, Boland, Alexander, Zagzag, Yancopoulos and Wiegand (1999); Döme, Paku, Somlai and Tímár (2002); Küsters, Leenders, Wesseling, Smits, Verrijp, Ruiter, Peters, van der Kogel and de Waal (2002); Döme, Hendrix, Paku, Tóvári and Timar (2007)]. The experimental results reported by Holash, Maisonpierre, Compton, Boland, Alexander, Zagzag, Yancopoulos and Wiegand (1999) showed that even the smallest C6 gliomas at just 1 week after implantation were well vascularized by cooption of pre-existing vessels. These coopted host vessels do not immediately undergo angiogenesis but instead regression, leading to a secondarily avascular tumour and massive tumour cell loss. Although the vascularization model of coopting host vessel remains controversial [Vajkoczy, Farhadi, Gaumann, Heidenreich, Erber, Wunder, Tonn, Menger, Breier et al. (2002)], information on the initial interplay between tumour cells and pre-existing vasculature may help develop strategies for prevention and treatment of metastases.

Tumour micrometastases and invasion require chemotactic migration of cancer cells, steered by protrusive activity of cell membrane and its attachment to the extracellular matrix (ECM) [Yamaguchi, Wyckoff and Condeelis (2005)]. In addition, many experimental studies have described the early growth of tumour cell along pre-existing vessels. Carbonell, Ansorge, Sibson and Muschel (2009) hypothesized the vascular basement membrane as the active substrate for tumour cell growth in the brain, and proposed that the interactions with the pre-existing vessels are required for initial cancer cell adhesion, proliferation and invasion. Zhao, Yang, Shi, Wang, Chen, Yuan, Lin and Wei (2011) clearly observed that tumour cells coopted, migrated along and proliferated on the surface of host vessels at an early stage after they extravasated from host vessels, using metastatic microtumour models in

transgenic zebrafish. Moreover, the distinct contributions of vessel cooption and angiogenesis during the initiation of microtumours and micrometastases were discussed in their study. Kienast, von Baumgarten, Fuhrmann, Klinkert, Goldbrunner, Herms and Winkler (2010) used multiphoton laser scanning microscopy to image the single steps of metastasis formation in real time, including arrest at vascular branch points, early extravasation, migration along microvessels and perivascular growth by vessel cooption.

Despite the tremendous advances in *in vivo* imaging techniques of animal models, mathematical modelling contributes greatly in improving our understanding of initial micrometastases formation and its interactions with local microenvironments. Early stage models were generally of the simulation of single phenomena, such as cell migration and invasion through the ECM [Anderson (2005); Lolas (2006); Painter (2009)]. The dynamic interactions of tumour cell evolution with the coupling of pre-existing vessels and host microenvironments are the main focuses in recent works. Welter, Bartha and Rieger (2008, 2009) studied the influence of heterogeneous tumour vasculature on the oxygen transport, drug delivery and ultimate tumour growth. In our previous work [Cai, Xu, Wu and Long (2011)], we proposed a coupled mathematical modelling system to investigate the dynamic process of tumour cell proliferation, death and tumour angiogenesis by fully coupling the vessel growth, tumour growth and blood perfusion. Based on the coupling model, it is possible to not only study the influence of certain parameters or variation on the whole dynamic process to the overall tumour growth, but also remove some superimposed assumptions. However, the tumour growth and cooption with pre-existing vessel network at the initial early stage were not included in the model generation. Here, we want to focus on the initial microtumour and micrometastases formation by including cancer cell migration and host vessel cooption in the proposed coupled model. Migrating cells are included as a new phenotype to describe the migration behaviour of malignant tumour cells. Different migration abilities are assumed to reflect the adhesion of cell-cell, cell-matrix and cell-vessel. Pre-existing vessel cooption and remodelling are introduced according to the local haemodynamical microenvironment. After the tumour cells and tumour vessels distribution are updated, the chemical substances including oxygen, vascular endothelial growth factors (VEGFs), extra-cellular matrix (ECM) and matrix degradation enzymes (MDEs) are coupled calculated with the haemodynamical environment. A three-dimensional simulation region with parallel distributed host vessels is designed to reproduce the experimental results [Zhao, Yang, Shi, Wang, Chen, Yuan, Lin and Wei (2011)] for initial micrometastases formation. In addition, the influences of the ability of cell migration and the inclusion of vessel cooption on the formation of micrometastases are presented and discussed.

2 Description of the model system

2.1 Definition of elements and pre-existing vessel network

A basic grid of $100 \times 100 \times 100$ is generated uniformly within a cube simulation domain Ω of 1mm^3 (Figure 1). The lattice constant is $10\mu\text{m}$, which is of the order of the typical diameter of tumour cells. Each site can be occupied by a single tumour cell or an endothelial cell. Unoccupied space is part of the ECM and/or healthy tissue. 25 arterioles with uniform diameter of $8\mu\text{m}$ are distributed parallel approximately, to form the network of pre-existing vasculature (as shown in red tubes in Figure 1).

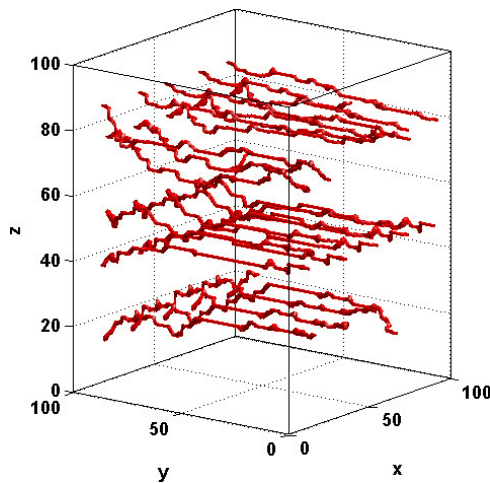


Figure 1: Illustration of simulation domain. Pre-existing vessel network is represented by red tubes.

2.2 Tumour cell behaviour

We assumed four different phenotypes of tumour cells: the proliferative cells (PC), the quiescent cells (QC), the necrotic cells (NC) and the migrating cells (MC). Two thresholds of oxygen concentration for cell proliferation (θ_{prol}) and cell survival (θ_{surv}) are introduced to describe the effects of oxygen field on the tumour cell actions. The detailed definitions of the relationships of the first three phenotypes of tumour cells with the local microenvironment can be found in our published paper [Cai, Xu, Wu and Long (2011); Cai, Zhang, Wu and Li (2015)]. Each phenotype of tumour cell has a different coefficient of oxygen consumption rate and the production rate of VEGF and MDEs (Table 1).

Table 1: Parameters of different phenotypes of tumour cells.

Phenotypes	MDE production	VEGF production	Oxygen consumption
Migrating cells (MC)	$2\mu_T$	$\chi \times 4$	2γ
Proliferating cells (PC)	μ_T	χ	γ
Quiescent cells (QC)	$\mu_T/5$	$\chi \times 2$	$\gamma/2$
Necrotic cells (NC)	$\mu_T/10$	$\chi \times 4$	$\gamma/4$

To model the cell migration through the matrix and along the pre-existing vessels in the early stage of microtumour growth, a specific phenotype, called the migrating cell (MC), is assumed. When local oxygen level is higher than θ_{surv} but lower than θ_{prol} and a space is available, a proliferating cell has a probability (50%) to become a migrating cell. Each neighbouring element of a MC has a probability defined as p_m to determine the migrating direction of the MC. p_m is related with the local oxygen concentration c_o and ECM concentration c_f ,

$$p_m = \delta_o c_o - \delta_f c_f \tag{1}$$

where δ_o and δ_f are the weights of influence of oxygen and ECM distributions on MCs. In other word, a MC is more likely to move towards a neighbouring space which has the high oxygen concentration and low ECM concentration in the neighbouring elements. In addition, it was also assumed that the MCs adjacent to the pre-existing vessel wall have higher probability of moving in the longitudinal direction (vessel axial direction) than the radial direction. The migration speeds of the two directions are the same, i.e., $10\mu\text{m}$ per time step. After a MC completes its movement, the space it originally occupied will be released for other cells.

2.3 Pre-existing vessel cooption, remodelling and angiogenesis

In this model, we consider vessel dilation as the first sign of a pre-existing vessel becoming a coopted vessel. A vessel segment surrounded by tumour cells has a VEGF concentration larger than a threshold θ_{VEGF} will increase its radius R with the rate of $0.4\mu\text{m/h}$, which will stop when the vessel radius reaches the maximum value of $R_{\text{max}} = 10\mu\text{m}$. At the same time, the permeability of the vessel wall L_p is increasing in a coopted vessel, and satisfies

$$L_p = \begin{cases} L_p^T \left(1 - \frac{R_{\text{max}} - R}{R_{\text{max}}} \right), & \text{coopted vessel} \\ L_p^N, & \text{mature vessel} \end{cases} \tag{2}$$

where L_p^N is the initial value of L_p referred to the vessel permeability value in the normal tissue; L_p^T is the maximum value of L_p according to the experiments of vessel permeability value in a tumour microvessel.

In the simulation, vessel wall compliance is defined by the radius changing under the influence of intravascular and interstitial pressures and collapse pressure based on the empirical equation of Netti, Roberge, Boucher, Baxter and Jain (1996).

$$R = \begin{cases} R_0 \left(\frac{P_v - P_i + P_c}{E} \right)^b, & \text{immature vessel} \\ R_0, & \text{mature vessel} \end{cases} \quad (3)$$

where R_0 is the origin radius of the capillary; b is the compliance exponent; E is the compliance coefficient. The intravascular and interstitial pressures are calculated by fully coupled haemodynamic simulation, which will be detailed in Section 2.4.

Based on the above equations, when the vessel segment becomes coopted, L_p will increase which causes higher P_i , and consequently vessel will be compressed. A compressed vessel, on the other hand will induce a higher flow resistance, lower flow which will then decrease the wall shear stress (WSS) level for the vessel. Vessel collapse will occur by either a significant reduced R or WSS criteria [Dimmeler and Zeiher (2000)].

Endothelial sprouting is allowed in tumour vessels if the local VEGF is high enough. The endothelial cell distribution is updated following the equation

$$\frac{\partial e}{\partial t} = D_e \nabla^2 e - \nabla \cdot \left(\frac{\phi_c}{1 + \sigma C_v} e \nabla C_v + \phi_h e \nabla C_f \right) \quad (4)$$

where e is the EC density. D_e , ϕ_c , ϕ_h are EC diffusion, chemotaxis and haptotaxis coefficients, respectively. The hybrid discrete-continuum technique [Anderson and Chaplain (1998)] is used to follow the path of an individual endothelial cell and generate the angiogenic vessel network.

2.4 Microenvironment

Tumour cell behaviour and tumour vessel remodelling are dynamically coupled by the changes of local microenvironment, including chemical substances and haemodynamics. The transport of the chemicals (oxygen, VEGF and MDEs) are modelled by quasi-steady reaction-diffusion equations. VEGF is assumed to diffuse, decay and be consumed by angiogenic sprouts. The production of VEGF is assumed to be proportional to TCs and ECM, representing the secretion of VEGF by TCs and the up-regulated level of VEGF in the ECM. The ECM is treated as a continuous

substance and can be degraded by MDEs, while the MDEs are governed by diffusion, produced by TCs and ECs, and the decay of itself. The equations of chemicals concentration are given as follows,

$$\frac{\partial C_v}{\partial t} = D_v \nabla^2 C_v + \chi TC_{i,j} + \xi C_f - \varepsilon EC_{i,j} - \theta C_v \quad (5)$$

$$\frac{\partial C_f}{\partial t} = -\delta C_m C_f \quad (6)$$

$$\frac{\partial C_m}{\partial t} = D_m \nabla^2 C_m + \mu_T TC_{i,j} + \mu_E EC_{i,j} - \lambda C_m \quad (7)$$

where C_v , C_f and C_m are the VEGF, ECM and MDE concentration, respectively. The $TC_{i,j}$ and $EC_{i,j}$ terms represent a tumour cell and an endothelial cell located at a node position (i, j) . Their values are either 1 if a cell is present or 0 if it is not. D_v is VEGF diffusion coefficient. D_m is the MDE diffusion coefficient. χ , ξ , ε , θ , δ , μ_T , μ_E and λ are positive constants.

To obtain a more realistic oxygen concentration field, the advection and diffusion of oxygen in the vessel network are introduced, based on the work of Fang, Sakadzic, Ruvinskaya, Devor, Dale and Boas (2008). The computational space is separated into three domains to characterize three distinct physiological processes, which are (a) the oxygen advection equation inside the vessel, (b) the oxygen flux across the vessel wall and (c) the free oxygen diffusion in the tissue. The detailed equations and descriptions of oxygen transport can be found in Cai, Zhang, Wu and Li (2015).

The haemodynamic model in this study is based on our previous work on the coupled modelling of intravascular blood flow with interstitial fluid flow [Wu, Long, Xu and Padhani (2009); Wu, Cai, Xu, Long, Ding and Dong (2012)]. Briefly, the basic equation for the intravascular blood flow is the flux concentration and incompressible flow at each node. Flow resistance is assumed to follow Poiseuille's law in each vessel segment. The interstitial fluid flow is controlled by Darcy's law. The intravascular and interstitial flow is coupled by the transvascular flow, which is described by Starling's law. Blood viscosity is a function of vessel diameter, local haematocrit, and plasma viscosity [Pries and Secomb (2005)]. In addition, vessel compliance and wall shear stress are correlated to vessel remodelling and vessel collapse (see Section 2.3).

The main equations for blood flow calculation are as follows:

$$Q_v = \frac{\pi R^4 \Delta P_v}{8 \mu \Delta l} \quad (8)$$

$$Q_t = 2\pi R \cdot \Delta l \cdot L_p (P_v - P_i - \sigma_T (\pi_v - \pi_i)) \quad (9)$$

$$Q = Q_v - Q_t \quad (10)$$

where Q is the flow rate of each vessel segment, which has a value zero at each node of the vessel network due to the assumption of flux conservation and incompressible flow. Q_v is the vascular flow rate without fluid leakage; Q_t is the transvascular flow rate. Δl and R are the mean length and radius of the vessel segment. P_v and P_i are the intravascular pressure and the interstitial pressure, respectively. L_p is the hydraulic permeability of the vessel wall. σ_T is the average osmotic reflection coefficient for plasma proteins; π_v and π_i are the colloid osmotic pressure of plasma and interstitial fluid, respectively. The total difference of P_v from plane $y = 100$ to $y = 0$ is set to be 3.5mmHg as the driving force of blood in the network (or the boundary condition).

The velocity of intravascular U_v and interstitial flow U_i satisfies

$$U_v = Q/\pi R^2 \quad (11)$$

$$U_i = -K\nabla P_i \quad (12)$$

$$\nabla \cdot U_i = \frac{L_p S}{V} (P_v - P_i - \sigma_T (\pi_v - \pi_i)) \quad (13)$$

where K is the hydraulic conductivity coefficient of the interstitium; S/V is the surface area per unit volume for transport in the interstitium.

From the haemodynamic simulation, we are able to obtain (a) intravascular flow velocity U_v and the haematocrit H in the microvessel network which are used in the oxygen concentration calculation, and (b) vessel diameter which is used to estimate vessel remodelling and collapse.

2.5 Setup of basic model

The initial condition of ECM density is set to be 1 and other chemicals' concentration (oxygen, VEGF and MDEs) are 0. No-flux boundary conditions are used in the simulation field. Since chemicals are transported much faster than the characteristic time for cell proliferation and migration, the chemicals' concentrations are solved to steady state at each time step of the simulation with an inner iteration step of 5s. As the tumour grew with time, the concentrations of chemical substances such as oxygen, VEGF, ECM and MDEs are calculated accordingly. At the same time, tumour vessels undergo remodelling and collapse in response to both chemical environment and haemodynamical environment. As a consequence, the local oxygen supply changes with the updated tumour vasculature, which determines the different phenotypes of tumour cells in next time step.

In the basic model, the weights of influence of oxygen and ECM distributions on MCs are equal, i.e., δ_o and δ_f are both set to be 0.5. Initially, 10 proliferating cells are placed around the pre-existing vessel in the central computational area.

Simulation stopped after angiogenesis phase occurred. In Table 2, all parameter values of the base case scenario are summarized.

3 Simulation results

3.1 Basic case scenario

3.1.1 General tumour morphology

Figure 2 showed the three-dimensional global pictures of tumour morphology and vessel network at different time phases during the growth period. It clearly indicated that tumour cells migrate and proliferate along the pre-existing vessels at the very early stage of growth ($T = 20$). Scattered distributed micrometastases occurred in the surrounding tissue at $T = 50$. These micrometastatic foci underwent further proliferation and ultimately formed dendritic invasion pattern, which can be seen at $T = 100$. Due to the limited oxygen supply by the pre-existing vessels, angiogenesis phase occurred at $T = 120$. The angiogenic vessels generated a new supply of oxygen for further tumour growth, resulting in exponential tumour cell proliferation (also refer to the growth history curve of basic case in Figure 6). Note the vessel dilation indicated by the enlarged vessel diameters at $T = 150$.

3.1.2 Detailed cell migration and vessel cooption

To study the interactions of tumour cells with host vessels at the very early stage of growth, the horizontal views of the three-dimensional global pictures at plane $z = 50$ were shown in Figure 3. The initial injected cells (pink dots) migrated and coopted the pre-existing vessels. The maximum longitudinal migration distance was up to $150 \mu\text{m}$ from the primary site at $T = 20$. No obvious tumour-induced angiogenesis was observed during this process. The coopted host vessels also became abnormal, with vessel dilation (indicated by light white) and increased vessel wall permeability, which would change the local haemodynamical and chemical microenvironment to influence the microtumour growth. At $T = 30$, a cluster of micrometastases can be seen clearly in the region closest to the pre-existing vessel. At the same time, the microtumour growth in longitudinal direction had been decreased, while the growth in transverse direction significantly accelerated. More and more micrometastases were observed in the simulation region at $T = 40$. Most migrating cells distributed along the pre-existing vessels; however, there were plenty of scattered tumour cells in the tissue region.

3.1.3 Comparison with experimental results

We have reproduced the experimental observations of initial microtumour growth in above results, including: (a) tumour cells proliferate, migrate and coopt with

Table 2: Parameter values used in the simulation.

Parameter	Value	Description	Reference
Δl	10 μ m	Lattice constant	Estimated
σ_T	0.82	Average osmotic reflection coefficient for plasma proteins	Baxter and Jain (1989)
π_v	20mmHg	Colloid osmotic pressure of plasma	Baxter and Jain (1989)
π_i	15mmHg	Colloid osmotic pressure of interstitial fluid	Baxter and Jain (1989)
K	4.13 $\times 10^{-8}$ cm ² /mmHg·s	Hydraulic conductivity coefficient of the interstitium	Baxter and Jain (1989)
S/V	200cm ⁻¹	Surface area per unit volume for transport in the interstitium	Baxter and Jain (1989)
D_m	10 ⁻⁹ cm ² s ⁻¹	MDE diffusion coefficient	Anderson (2005)
δ	1.3 $\times 10^2$ cm ³ M ⁻¹ s ⁻¹	ECM degradation coefficient	Cai, Xu, Wu and Long (2011)
μ_T	1.7 $\times 10^{-18}$ Mcells ⁻¹ s ⁻¹	MDE production by TC	Cai, Xu, Wu and Long (2011)
μ_E	0.3 $\times 10^{-18}$ Mcells ⁻¹ s ⁻¹	MDE production by EC	Cai, Xu, Wu and Long (2011)
λ	1.7 $\times 10^{-8}$ s ⁻¹	MDE decay coefficient	Anderson (2005)
D_v	2.9 $\times 10^{-7}$ cm ² s ⁻¹	VEGF diffusion coefficient	Anderson and Chaplain (1998)
χ	10 ⁻¹⁷ Mcells ⁻¹ s ⁻¹	VEGF production by TC	Alarcón, Owen, Byrne and Maini (2006)
ξ	10 ⁻³ cm ⁻³ s ⁻¹	VEGF production in ECM	Fang, Sakadzic, Ruvinskaya, Devor, Dale and Boas (2008)
ε	10 ⁻²⁰ Mcells ⁻¹ s ⁻¹	VEGF consumption by EC	Alarcón, Owen, Byrne and Maini (2006)
θ	10 ⁻⁸ s ⁻¹	VEGF decay coefficient	Alarcón, Owen, Byrne and Maini (2006)
L_p^T	2.8 $\times 10^{-7}$ cm/mmHg·s	Vessel permeability in tumour tissue	Baxter and Jain (1989)
D_e	10 ⁻⁹ cm ² s ⁻¹	EC diffusion coefficient	Anderson and Chaplain (1998)
ϕ_c	2.6 $\times 10^3$ cm ² M ⁻¹ s ⁻¹	EC chemotaxis coefficient	Anderson and Chaplain (1998)
ϕ_h	10 ³ cm ² M ⁻¹ s ⁻¹	EC haptotaxis coefficient	Anderson and Chaplain (1998)
E	6.5mmHg	Vessel compliance coefficient	Netti, Roberge, Boucher, Baxter and Jain (1996)
b	0.1	Vessel compliance index	Netti, Roberge, Boucher, Baxter and Jain (1996)

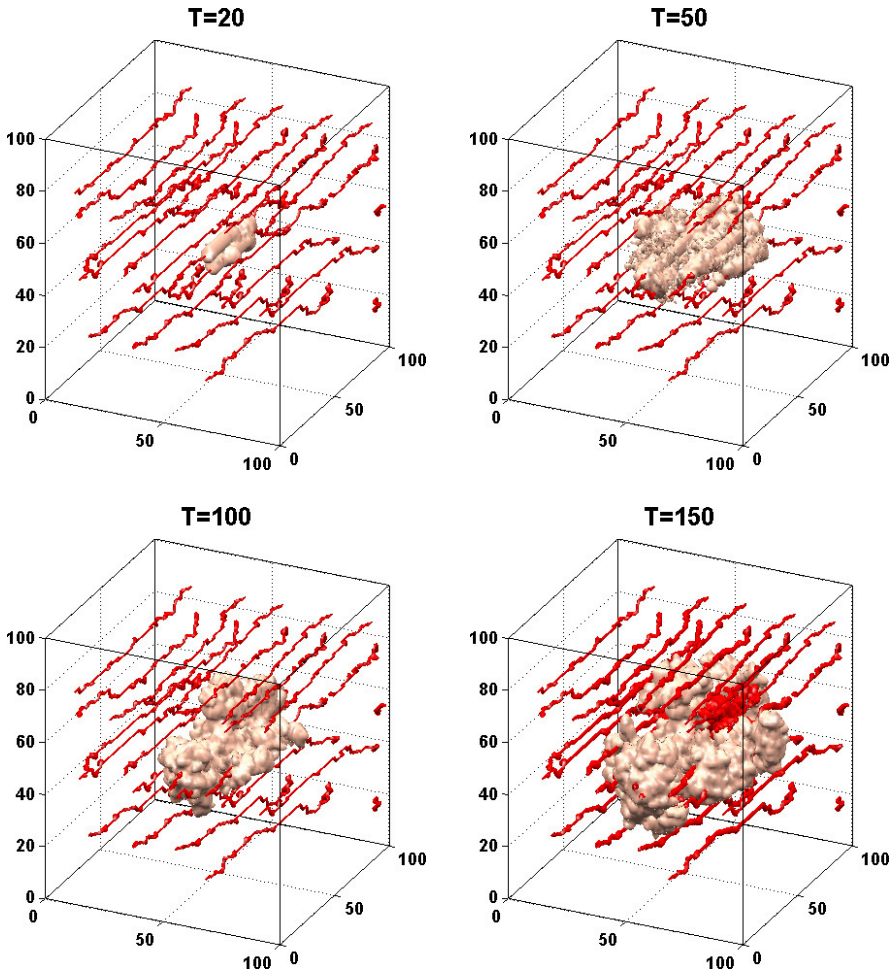


Figure 2: Tumour morphology at different simulation time. The microvasculature is represented by red tubes.

the pre-existing vessels; (b) the coopted vessels in turn influence the tumour cell growth by changing the local microenvironment. To further these findings, we analyzed the tumour growth speed in longitudinal and vertical directions quantitatively (Figure 4). The results showed that the growth speed in longitudinal direction significantly exceeded the expansion in transverse direction. In addition, the increase of angiogenic vessels in microtumour accelerated the growth in vertical direction while decreased the growth in longitudinal direction. This was consistent with the

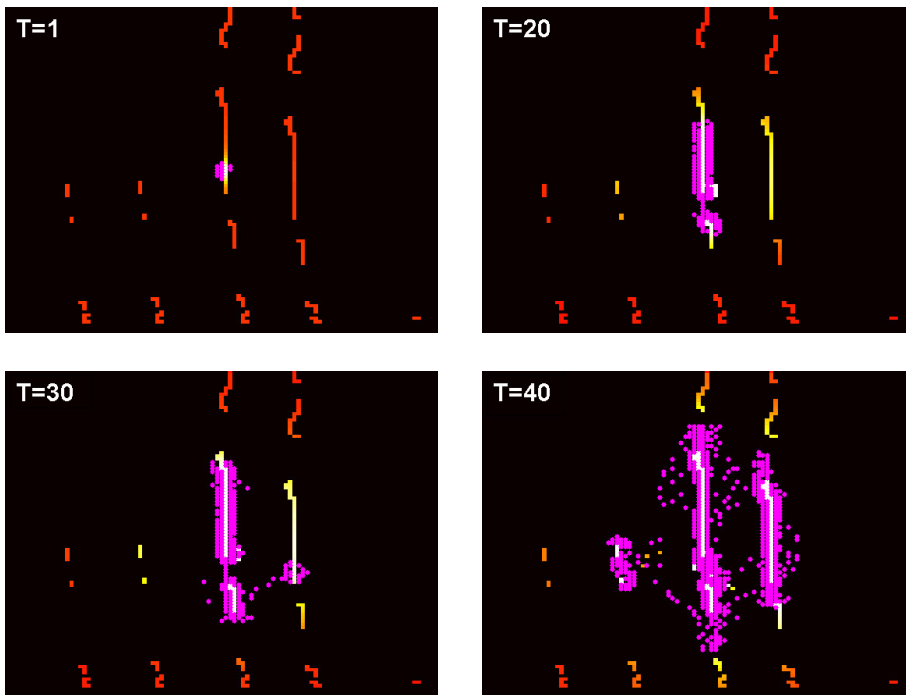


Figure 3: The horizontal views of Figure 2 at plane $z=50$. Pink dots represent active tumour cells. Light parts in the vessels indicate the vessel dilation.

experimental results observed by Zhao, Yang, Shi, Wang, Chen, Yuan, Lin and Wei (2011).

3.2 Model variations

3.2.1 Migration ability

More simulations were performed to test the influence of different cell migration ability on the final tumour morphology. In the current model, the migration probability p_m of a MC is determined by δ_o and δ_f , which are the weights of influence of oxygen and ECM distributions on MCs, respectively. In the basic model, the two parameters δ_o and δ_f was set to equal. In the test models (Figure 5), we found that tumours with high δ_o develop a dendritic morphology with cauliflower-like invasion into healthy tissue; however, tumours with high δ_f are more likely to develop a rounded morphology with scattered micrometastases. This result identified the important role of the cell migration ability for the patterns of micrometastases.

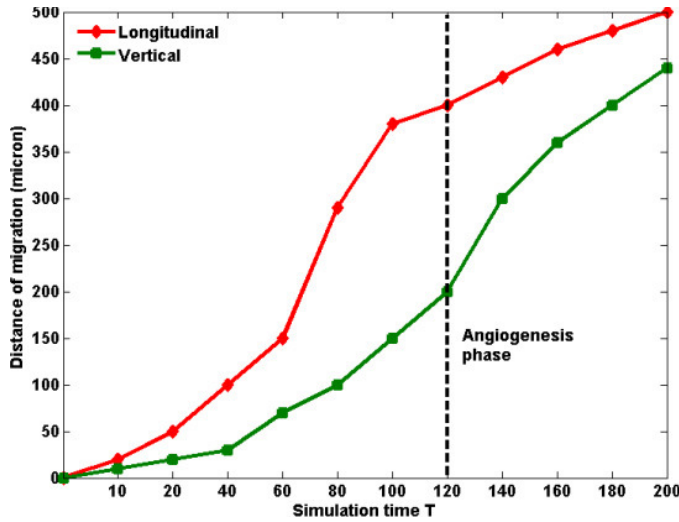


Figure 4: Quantitative analysis of the tumour expansion in longitudinal and vertical directions. The results showed that the growth speed in longitudinal direction (red line) significantly exceeded the expansion in transverse direction (green line).

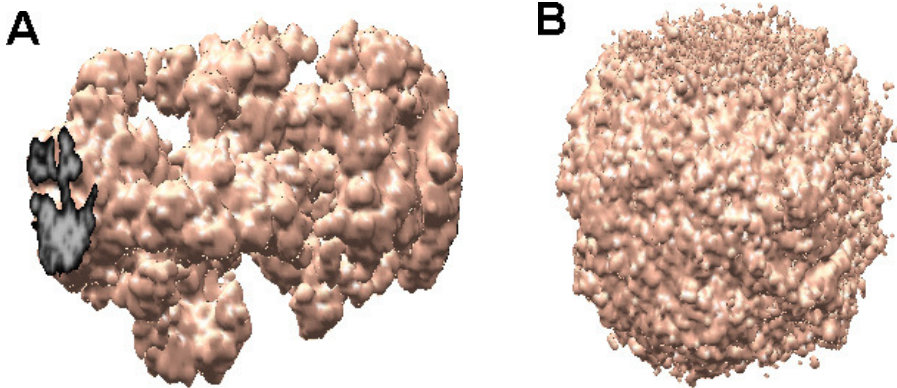


Figure 5: Tumour morphology influenced by the different cell migration ability. A. $\delta_o = 0.8$ and $\delta_f = 0.2$. Tumours develop a dendritic morphology with cauliflower-like invasion into healthy tissue. B. $\delta_o = 0.2$ and $\delta_f = 0.8$. Tumours develop a rounded morphology with scattered micrometastases.

3.2.2 Vessel cooption

In the current model, vessel dilation is the first sign of a pre-existing vessel becoming a coopted vessel, leading to a cascade process. Since the key parameters of

this remodelling are initiated by the changing in L_p and P_c , the constant R , L_p and P_c were used in the test model, which means the vessel cooption and remodelling were neglected. The growth history curves of tumour mass with (Basic case) and without (Test case) vessel cooption were shown in Figure 6. Although there was no significant difference in the growth trend between the two cases, the angiogenesis phase occurred earlier with cut-off of the vessel cooption and remodelling. This indicated that tumour cells would coopt pre-existing host vessels to acquire sufficient oxygen to survive before inducing angiogenic sprout.

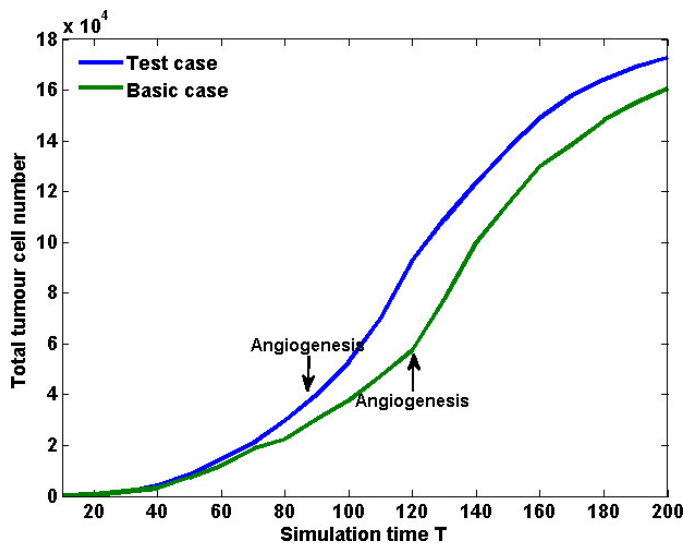


Figure 6: Growth history curves of tumour mass with (Basic case) and without (Test case) vessel cooption. Arrows indicate the starting point of angiogenesis phase.

4 Discussion and conclusion

The present study provides the detailed quantitative analyses of initial microtumour and micrometastases formation by including cancer cell migration and host vessel cooption in the proposed coupled model. Migrating cells are included as a new phenotype to describe the migration behaviour of malignant tumour cells. Migration probability p_m of a migrating cell is influenced by local microenvironment, such as oxygen and ECM distribution. Pre-existing vessel cooption and remodelling are introduced according to the local haemodynamical microenvironment. After the tumour cells and tumour vessels distribution are updated, the chemical substances are coupled calculated with the haemodynamical environment.

The model demonstrates the growth process of microtumours and initial micrometastases formation. The simulation results clearly reproduce the tumour cells migrate and proliferate along the pre-existing vessels at the very early stage of growth, which are consistent with many published experimental observations. In addition, the coopted host vessels become abnormal, with vessel dilation and increased vessel wall permeability, leading to the changes in local haemodynamical and chemical microenvironment. These interactions of tumour cells with the pre-existing vessels are believed to be essential for initial adhesion, proliferation, invasion, and micrometastases establishment [Carbonell, Ansorge, Sibson and Muschel (2009)]. Quantitative analysis of tumour growth in longitudinal and vertical directions have shown that the growth in longitudinal direction will decrease while the growth in transverse direction will increase in angiogenesis phase. In other word, the cooption and migration along host vessels would be inhibited once angiogenesis began to be induced.

To study the influence of the ability of cell migration and the inclusion of vessel cooption on the formation of micrometastases, more simulations have carried out. The results have shown the different patterns of micrometastases with different cell migration ability, which suggest that the role of cell migration is noteworthy in the tumour pathological research and therapies. Moreover, we found that the angiogenesis phase occurred earlier with cut-off of the vessel cooption and remodelling. We can deduce that tumour cells would coopt pre-existing host vessels to acquire sufficient oxygen to survive before inducing angiogenic sprout.

Herein we used the migration direction probability of MCs to model the migrating behaviour of a tumour cell. The setting was quite rough, since it was our first attempt to establish the coupling system between cell migration with the local microenvironment. The influences of different cell migration ability on the final tumour morphology have been discussed. We are going to extend the current model to incorporate certain signaling pathway in the sub-cellular level, which is linked to a cell-cycle pathway to determine the cell phenotype.

It is our aim to simulate the tumour growth and cooption with pre-existing vessel network at the initial early stage of micrometastases formation. By using the coupled model of cell migration, vessel cooption and tumour microenvironment, it is possible to study the dynamic interactions between tumour cells with host vessels. Furthermore, the tumour morphology and micrometastases patterns may vary by variables in the model. Being comprised of different model settings that are easily modified, the presented model has the potential to be customized for specific tumours and microenvironment.

Conflict of interest

The authors declare that there is no conflict of interest regarding the publication of this manuscript.

Acknowledgement: This research is supported by the National Basic Research Program of China (973 Program) (No. 2013CB733800), the National Nature Science Foundation of China (No. 11302050, No. 11272091), the Nature Science Foundation of Jiangsu Province (No. BK20130593).

References

Alarcón, T.; Owen, M. R.; Byrne, H. M.; Maini, P. K. (2006): Multiscale modelling of tumour growth and therapy: the influence of vessel normalisation on chemotherapy. *Computational and Mathematical Methods in Medicine*, vol. 7, no. 2-3, pp. 85–119.

Anderson, A. R. (2005): A hybrid mathematical model of solid tumour invasion: the importance of cell adhesion. *Math. Med. Biol.*, vol. 22, no. 2, pp. 163–186.

Anderson, A. R.; Chaplain, M. (1998): Continuous and discrete mathematical models of tumor-induced angiogenesis. *Bulletin of mathematical biology*, vol. 60, no. 5, pp. 857–899.

Baxter, L. T.; Jain, R. K. (1989): Transport of fluid and macromolecules in tumors. i. role of interstitial pressure and convection. *Microvascular research*, vol. 37, no. 1, pp. 77–104.

Cai, Y.; Xu, S.; Wu, J.; Long, Q. (2011): Coupled modelling of tumour angiogenesis, tumour growth and blood perfusion. *Journal of Theoretical Biology*, vol. 279, no. 1, pp. 90–101.

Cai, Y.; Zhang, J.; Wu, J.; Li, Z.-y. (2015): Oxygen transport in a three-dimensional microvascular network incorporated with early tumour growth and preexisting vessel cooption: Numerical simulation study. *BioMed research international*, vol. 2015.

Carbonell, W. S.; Ansorge, O.; Sibson, N.; Muschel, R. (2009): The vascular basement membrane as “soil” in brain metastasis. *PloS one*, vol. 4, no. 6, pp. e5857.

Dimmeler, S.; Zeiher, A. M. (2000): Endothelial cell apoptosis in angiogenesis and vessel regression. *Circulation research*, vol. 87, no. 6, pp. 434–439.

Döme, B.; Hendrix, M. J.; Paku, S.; Tóvári, J.; Timar, J. (2007): Alternative vascularization mechanisms in cancer: Pathology and therapeutic implications. *The American journal of pathology*, vol. 170, no. 1, pp. 1–15.

Döme, B.; Paku, S.; Somlai, B.; Tímár, J. (2002): Vascularization of cutaneous melanoma involves vessel co-option and has clinical significance. *The Journal of pathology*, vol. 197, no. 3, pp. 355–362.

Fang, Q.; Sakadzic, S.; Ruvinskaya, L.; Devor, A.; Dale, A. M.; Boas, D. A. (2008): Oxygen advection and diffusion in a three-dimensional vascular anatomical network. *Optics express*, vol. 16, no. 22, pp. 17530–17541.

Folkman, J. (1971): Tumor angiogenesis: therapeutic implications. *New England Journal of Medicine*, , no. 285, pp. 1182–6.

Folkman, J. (2003): Angiogenesis and apoptosis. In *Seminars in cancer biology*, volume 13, pp. 159–167. Elsevier.

Holash, J.; Maisonpierre, P.; Compton, D.; Boland, P.; Alexander, C.; Zagzag, D.; Yancopoulos, G.; Wiegand, S. (1999): Vessel cooption, regression, and growth in tumors mediated by angiopoietins and vegf. *Science*, vol. 284, no. 5422, pp. 1994–1998.

Kienast, Y.; von Baumgarten, L.; Fuhrmann, M.; Klinkert, W. E.; Goldbrunner, R.; Herms, J.; Winkler, F. (2010): Real-time imaging reveals the single steps of brain metastasis formation. *Nature medicine*, vol. 16, no. 1, pp. 116–122.

Küstners, B.; Leenders, W. P.; Wesseling, P.; Smits, D.; Verrijp, K.; Ruiter, D. J.; Peters, J. P.; van der Kogel, A. J.; de Waal, R. M. (2002): Vascular endothelial growth factor- α 165 induces progression of melanoma brain metastases without induction of sprouting angiogenesis. *Cancer research*, vol. 62, no. 2, pp. 341–345.

Lolas, G. (2006): Mathematical modelling of proteolysis and cancer cell invasion of tissue. In *Tutorials in Mathematical Biosciences III*, pp. 77–129. Springer.

Netti, P. A.; Roberge, S.; Boucher, Y.; Baxter, L. T.; Jain, R. K. (1996): Effect of transvascular fluid exchange on pressure–flow relationship in tumors: a proposed mechanism for tumor blood flow heterogeneity. *Microvascular research*, vol. 52, no. 1, pp. 27–46.

Painter, K. (2009): Modelling cell migration strategies in the extracellular matrix. *Journal of mathematical biology*, vol. 58, no. 4-5, pp. 511–543.

Pries, A. R.; Secomb, T. W. (2005): Microvascular blood viscosity in vivo and the endothelial surface layer. *American Journal of Physiology-Heart and Circulatory Physiology*, vol. 289, no. 6, pp. H2657–H2664.

Vajkoczy, P.; Farhadi, M.; Gaumann, A.; Heidenreich, R.; Erber, R.; Wunder, A.; Tonn, J. C.; Menger, M. D.; Breier, G. et al. (2002): Microtumor growth initiates angiogenic sprouting with simultaneous expression of vegf, vegf receptor-2, and angiopoietin-2. *The Journal of clinical investigation*, vol. 109, no. 109 (6), pp. 777–785.

Welter, M.; Bartha, K.; Rieger, H. (2008): Emergent vascular network inhomogeneities and resulting blood flow patterns in a growing tumor. *Journal of theoretical biology*, vol. 250, no. 2, pp. 257–280.

Welter, M.; Bartha, K.; Rieger, H. (2009): Vascular remodelling of an arteriovenous blood vessel network during solid tumour growth. *Journal of theoretical biology*, vol. 259, no. 3, pp. 405–422.

Wu, J.; Cai, Y.; Xu, S.; Long, Q.; Ding, Z.; Dong, C. (2012): 3 d numerical study of tumor microenvironmental flow in response to vascular-disrupting treatments. *Molecular & Cellular Biomechanics*, vol. 9, no. 2, pp. 95–125.

Wu, J.; Long, Q.; Xu, S.; Padhani, A. R. (2009): Study of tumor blood perfusion and its variation due to vascular normalization by anti-angiogenic therapy based on 3d angiogenic microvasculature. *Journal of biomechanics*, vol. 42, no. 6, pp. 712–721.

Yamaguchi, H.; Wyckoff, J.; Condeelis, J. (2005): Cell migration in tumors. *Current opinion in cell biology*, vol. 17, no. 5, pp. 559–564.

Zhao, C.; Yang, H.; Shi, H.; Wang, X.; Chen, X.; Yuan, Y.; Lin, S.; Wei, Y. (2011): Distinct contributions of angiogenesis and vascular co-option during the initiation of primary microtumors and micrometastases. *Carcinogenesis*, vol. 32, no. 8, pp. 1143–1150.